Use of Artificial Potential Fields in the Exploration of Unknown Environments: Overcoming the Local Minimum Problem

Nathan Isaman
University of Washington
A A 510, Autumn 2017

Abstract*—Exploration is a critical task for most modern autonomous systems and doing so efficiently is essential. One common and computationally inexpensive method for autonomously exploring an unknown environment is the use of Artificial Potential Fields (APFs). Unexplored locations produce an attractive potential field while obstacles and explored spaces produce repulsive potential fields. The cumulative effect of these potential fields is an artificial force that directs a robot away from obstacles and towards new, unexplored regions. This paper introduces the fundamentals to constructing an APF as well as the most common and impactful shortfall of APFs: local minimums. A local minimum will, without external intervention, permanently halt exploration thereby ruining the entire exploration process. After addressing the source of local minimums, three independent modifications to the basic APF framework will be reviewed specifically regarding how local minimums were avoided. These modifications involve changes to the algorithm and subsequent introduction of virtual obstacles, implementation of Rotational Potential Fields (RPFs), and introduction of vorticity to otherwise linear repulsion field vectors.

I. Introduction

Significant amounts of research have been done on optimal path planning and navigation in known environments. The research cases always have an end goal location selected that must be reached and a number of obstacles and environmental geometries to work around. Solving this globally optimal motion planning problem, however, requires complete knowledge of the environment *a priori* and is not feasible otherwise. The topic of interest for this paper is the case where knowledge of the environment is not known and must be discovered through autonomous exploration. There is no ultimate goal location in mind, just the objective to fully and efficiently explore the space the robot is in. One method for exploring unknown environments is through the use of Artificial Potential Fields (APFs). APFs leverage the same mechanics seen with charged particles in an electromagnetic field; there are attractive and repulsive forces that affect the direction and speed of the particle of interest. The connection to the task of exploration is fairly straightforward: unknown regions are attractive while known regions and obstacles are repulsive. Other robots can also be assigned repulsive field effects to prevent collisions or promote dispersed exploration [4]. One important phenomenon every undergraduate STEM student runs into during their physics courses is the cancellation of opposing forces. In the case of APFs, this is manifest when the sum of attractive and repulsive forces on the robot are equal in magnitude and direction. Such cancellations halt exploration and trap the exploring robot in a region. This phenomenon, referred to as the local minimum problem, and the recent efforts to combat it are the focus of this paper.

II. Background

A. Basic Components of APFs

This section will cover the fundamental equations used to construct an APF. The two main components are the attractive and repulsive potentials [3]:

$$U_{att}(q, q_i) = \frac{1}{4} h_{att}(c) \rho_{goal}^4(q_i)$$

$$U_{rep}(q, q_i) = \begin{cases} \frac{1}{h_{rep}(c)} \left(\frac{1}{\rho(q)} - \frac{1}{\rho_0}\right)^2 & , \rho(q) \leq \rho_0 \\ 0 & , \rho(q) \geq \rho_0 \end{cases}$$

where $\rho(q)$ is defined using the Euclidean norm as seen below.

$$\rho(q) = \|q - q_i\|$$

These two functions are evaluated at the robot location q relative to the potentials at each other location q_i in the observed space. Different methods are used to split up and record a given space; [1] uses voxels in an OctoMap and [3] uses an occupancy grid. The maximum sensing distance for the robot is captured in the variable ρ_0 and the $h_{rep}(c)$ and $h_{att}(c)$ functions scale the potentials based on the coverage of the explored space. Most of the articles reviewed used either a linear scaling function or did not state how they scaled the potentials. Regarding the stated linear functions, [3] used the following:

$$h_{att}(c) = \frac{k_{att}}{c}$$

$$h_{rep}(c) = c k_{rep}$$

Now with the attractive and repulsive potentials defined, we can find the total potential at each location q_i and then take the gradient to determine the artificial force this total potential field exerts on the robot at its given location [1].

$$U_{total} = U_{att} + U_{rep}$$

$$F_{total} = F_{att} + F_{rep} = \bigtriangledown U_{total}$$

Useful equations for the attractive and repulsive forces that will be used in the following section can be found below [3].

$$F_{att} = \sum_{i=1}^{n} F_{att}(q, q_i) = \sum_{i=1}^{n} h_{att}(q_i - q)\rho_{goal}^2 \tag{1}$$

$$F_{rep} = \sum_{i=1}^{n} F_{rep}(q, q_i) =$$

$$= \sum_{i=1}^{n} \begin{cases} \frac{1}{2h_{rep}(c)}\left(\frac{1}{\rho(q)} - \frac{1}{\rho_0}\right)\frac{q-q_i}{\rho(q)^3} & ,\rho(q) \leq \rho_0 \\ 0 & ,\rho(q) \geq \rho_0 \end{cases} \tag{2}$$

B. The Local Minimum Problem

Now that the fundamental components of an APF are defined, the issue of a local minimum can be explored. As stated in the introduction, a local minimum occurs when the attractive and repulsive forces cancel each other at a given location.

$$0 = F_{att} + F_{rep} = \sum_{i=1}^{n}(F_{att}(q, q_i) + F_{rep}(q, q_i))$$

Substituting in equations (1) and (2) into the equation above, assuming $\rho(q) \leq \rho_0$ at all points considered yields:

$$0 = \sum_{i=1}^{n} h_{att}(c)(q_i - q)\rho_{goal}^2 + \frac{1}{2h_{rep}(c)}\left(\frac{1}{\rho(q)} - \frac{1}{\rho_0}\right)\frac{q-q_i}{\rho(q)^3}$$

$$0 = \sum_{i=1}^{n}(q_i - q)[h_{att}(c)\rho_{goal}^2 - \frac{1}{2h_{rep}(c)}\left(\frac{1}{\rho(q)} - \frac{1}{\rho_0}\right)\frac{1}{\rho(q)^3}]$$

Substituting in the definitions of $\rho(q)$, $h_{att}(c)$, and $h_{rep}(c)$ will provide some insight as to what is happening in the above equation. The scaling functions become scaling constants due to the cancellation of the c variable. This also means that the local minimums will persist regardless of the exploration progress and the commensurate variation in c.

$$0 = \sum_{i=1}^{n}(q_i - q)\left[k_{att}\|q_{goal} - q_i\|^2 - \frac{1}{2k_{rep}}\left(\frac{1}{\|q-q_i\|} - \frac{1}{\rho_0}\right)\frac{1}{\|q-q_i\|^3}\right]$$

The first term inside the summation above, $(q_i - q)$, represents the vector from the current robot location to another cell or voxel in the world representation. The second, scalar valued term represents the combination of attractive and repulsive forces in the observed space. If the maximum sensing distance is assumed to be extremely large, then the $1/\rho_0$ term will become negligible. This simplifying assumption turns the equation into:

$$\sum_{i=1}^{n}(q_i - q)\left(k_{att}\|q_{goal} - q_i\|^2 - \frac{1}{2k_{rep}\|q - q_i\|^4}\right) \tag{3}$$

Local minimums will occur at locations q where the sum of n terms in (3) results in zero. Not every q_i will have a repulsive or attractive magnitude therefore the scalar term in (3) does not generally involve both terms. Also, the vectors being summed leading to a zero result do not necessarily need to be attractive and repulsive respectively, two repulsive force vectors can cancel each other out if they are anti-parallel. Inspection of the scalar term in (3) reveals the primary conditions under which a single attractive and single repulsive force vector will cancel: when q_{goal} is far (enough) from some q and there is an obstacle at q_i near enough to q so that the norm $\|q - q_i\|$ is small. This will result in the repulsive element being large enough to counter the attractive element assuming both forces are along the same line of action. Also, borrowing from basic physics, it would seem to be especially likely to encounter these local minimums when exploring near the center of curvature of concave obstacles with a goal location on the opposite side. The repulsive force vectors coming from the obstacle surface would tend to cancel out one of the vector components at certain focal points, making it more likely to cause issues with an attractive force vector pointing toward the concave surface. This is the case seen in simulations conducted in [3] as seen in Figure 1 where the robot was trapped near the entrance to a C shaped room.

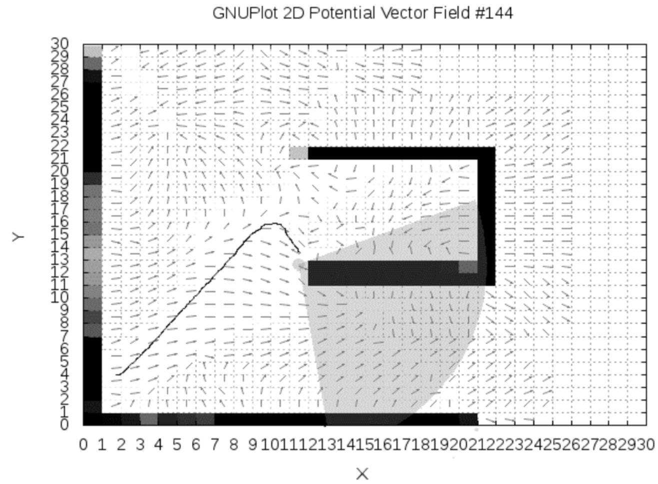

Fig. 1. Robot entrapment in local minimum using unmodified APF. Source: [3], Figure 2a

III. Recent Efforts to Overcome the Local Minimum Problem

Different methods developed in the last few years for overcoming the local minimum problem are presented in this section. The applications are generally concerned with reliability and efficient exploration.

A. Introduction of a Virtual Repulsive Obstacle

The local minimum avoidance method employed in [1] consists of an algorithmic and potential field adjustment compared to the standard APF implementation. A reward system was used to prevent the exploring agent from being trapped in a local minimum. For robot position $x_i \in X = [x_1, x_2, ..., x_n]$ and the reward at the previous m positions $\Delta = [\delta_1, \delta_2, ..., \delta_m]$, the reward at a certain point j can be calculated as:

$$\delta_j = \|x_i - x_{i-j}\|$$

where x_{i-j} represents the robot position in the j^{th} previous time-step. A result of $\delta_j = 0$ indicates that the robot has

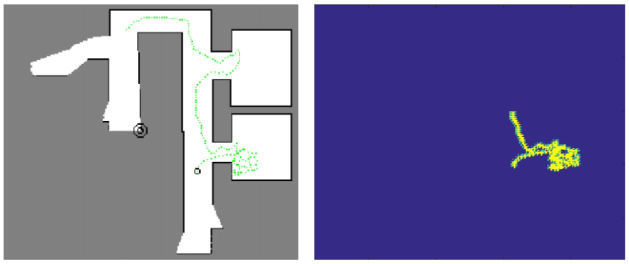

Fig. 2. Escape from a local minimum using a virtual repulsive obstacle. Source: [1], Figure 2a and 2b

been to that location before. Repeated δ_j values equal to zero indicate that the robot might be caught in a local minimum. The author defines U_{att} and U_{rep} as follows [1].

$$U_{att} = \gamma d^2(x_i, x_{goal})$$

$$U_{rep} = \zeta U_{obstacle} + \lambda U_{local}$$

where γ and ζ are weights, much like $h_{att}(c)$ and $h_{rep}(c)$ seen in the previous sections. The U_{local} term is caused by a virtual repulsive obstacle designed to assist the robot in escaping local minimum locations. The author defines the specific components $U_{obstacle}$ and U_{local} as the following:

$$U_{obstacle} = \frac{1}{\sum_k (x_i - c_k)^2}$$

$$U_{local} = \frac{\epsilon(k)}{\sum_k (x_i - c_k)^2}$$

where

$$\epsilon(k) = e^{-t/\tau} \sum_{j=1}^{m} \frac{1}{1+e^{-\|x_i^k - x_{i-j}^k\|}}$$

The second exponential term contains the reward variable δ_j so repeated visits to the same location c_k within a short time span results in the system viewing that specific location c_k as an obstacle and will then assign a repulsive potential to it [1]. The longer the robot stays in that area, the larger the magnitude of the repulsion becomes. Eventually this increase in magnitude will greatly imbalance the combined force magnitude term in (3) in favor of repulsion and send the robot along an appropriate escape vector regardless of attractive objects in the vicinity. The $\epsilon(k)$ function also contains a decaying time component so if the robot was temporarily trapped in a local minimum and the location c_k was made repulsive, the magnitude of the repulsion would decrease over time [1]. The time decaying repulsion of a local minimum location will not unnecessarily prevent the robot from moving into that region again to complete the exploration or depart an enclosed space. The result of this local minimization escape can be seen in Figure 2 [1]. The dense patch of yellow line in the second half of the figure represents entrapment of the robot in a local minimum. The rapidly revisited area became increasingly repulsive and eventually forced the robot out of the enclosed space back into the hallway.

B. Using a Rotational Potential Field Near Objects

The authors of [2] implemented Rotational Potential Fields (RPFs) near obstacles of surveying or mapping interest as a means to avoid entrapment by local minimums. Figure 3 illustrates the visual difference between a standard point obstacle with uniform, linear field lines to that of a rotational field around a point obstacle [2]. As with standard obstacles, the magnitude of the repulsion increases as distance to the obstacle decreases, something that is not clearly portrayed in Figure 3. It should be noted that the application interest in [2] is for Autonomous Underwater Vehicles (AUVs). The smaller number of obstacles in a much larger open space almost inverts the exploration problem. In this case, the exploration is of the obstacles discovered during transit. The idea behind RPFs is that the robot will be more helpfully guided around the obstacle by the tangential vectors without relying on the linear attractive and repulsive vectors summing to something similar in the standard case. One limitation of RPFs, outlined in [2], is that RPFs are inherently more efficient when implemented on a plane. This poses an issue when exploring 3D environments as an initial step after encountering an obstacle in the desired path is to superimpose a 2D plane intersecting the obstacle along a preferential axis. The RPF is then created on that 2D sub-plane and the robot is guided around it. The preferential orientation of the sub-plane is such that the normal vector of the plane is perpendicular to the robot's velocity vector on approach. This will ensure that the robot's trajectory around the object remains smooth regardless of what angle the approach is made at [2]. The authors of [2] used a 10 step process for generating and implementing the RPF on this sub-plane. The first five steps involve the creation of the three relative coordinate axes for the sub-plane using the assumed object's center as the new origin. The first unit vector, $\hat{\mathbf{t}}$, was created from the vector between the robot and the object center and the subsequent unit vectors, $\hat{\mathbf{b}}$ and $\hat{\mathbf{n}}$, were created from this one using the cross-product and standard vector normalization. In the end, a transformation matrix was formed out of these new local $\mathbf{R}^3$ basis vectors centered on the object [2]:

$$\mathbf{G} = \begin{bmatrix} \hat{t_x} & \hat{b_x} & \hat{n_x} \\ \hat{t_y} & \hat{b_x} & \hat{n_x} \\ \hat{t_z} & \hat{b_x} & \hat{n_x} \end{bmatrix}$$

Transformation of the robot's global position, P was then

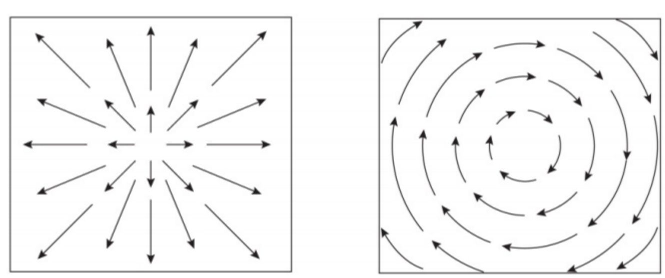

Fig. 3. Standard Potential Field vs Rotational Potential Field. Source: [2], Figure 1

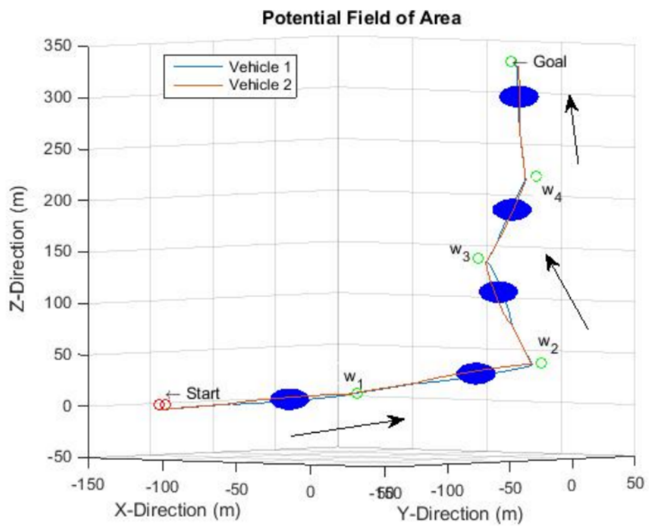

Fig. 4. Simulation Results using RPFs in 3D Environment. Source: [2], Figure 4

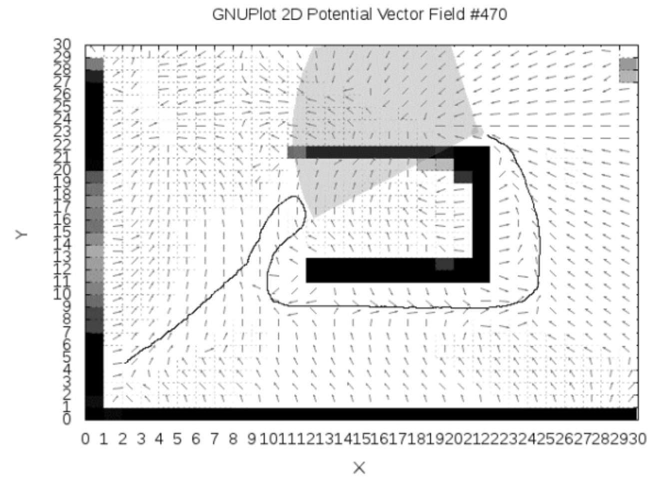

Fig. 5. 2D Exploration using modified APF. Source: [3], Figure 2b

converted to this new coordinate frame using the above transformation matrix as seen in the equation below.

$$\hat{\mathbf{P_s}} = \mathbf{G}\mathbf{P_s}$$

where $\mathbf{P_s}$ and $\hat{\mathbf{P_s}}$ are the positions of the robot relative to the object before and after transformation, respectively. This transformed coordinate basis was then used to implement the sub-plane RPF as a means to smoothly navigate the robot around the obstacle while avoiding any potential local minimums. The resultant force vector caused by the attractive goal location and the repulsive rotational field are very strongly directed around the object and should not result in entrapment for any spherical obstacles. The article did not discuss obstacles of differing geometries or large obstacles where determining a center and an appropriate orbit radius are more complex. Simulation results from [2] can be seen in Figure 4. Each unique sub-plane generated for each encountered object can be clearly seen by the trajectories of the two simulated robots. This method also resulted in smooth robot trajectories in addition to avoiding entrapment, despite the fact that the goal location was behind the repulsive object and very well could have resulted in a negation of force vectors on approach.

C. Introducing Vorticity to the Potential Field Near Obstacles

Similar to what was seen in [2] authors of [3] reduce the threat of local minimums by introducing some rotation to the potential fields near obstacles. Instead of defining a sub-plane and imposing a RPF, however, the authors of [3] introduce vorticity to the field via modification of (2) with the equations below:

$$(q - q_i) = (\|q - q_i\| R(\alpha)\hat{u})$$

where

$$R(\alpha) = \begin{bmatrix} \cos\alpha & -\sin\alpha \\ \sin\alpha & \cos\alpha \end{bmatrix}$$

and $\hat{u}$ is the unit vector of $(q - q_i)$ and α is the predetermined angle of twist for the vector field [3]. Equation (2) now becomes the following:

$$F_{rep}(q, q_i, \alpha) = \sum_{i=1}^{n} \begin{cases} \frac{1}{2h_{rep}(c)}\left(\frac{1}{\rho(q)} - \frac{1}{\rho_0}\right)\frac{(\|q-q_i\|R(\alpha)\hat{u})}{\rho(q)^3} & ,\rho(q) \leq \rho_0 \\ 0 & ,\rho(q) \geq \rho_0 \end{cases}$$

Repulsive force vectors will now always point away from the obstacle surface at an angle instead of potentially normal [3] to it for head-on approaches of flat walls or especially when exploring near or inside concave structures. Simulation results from [3] can be seen in Figure 5 where the vorticity of the vector field near the obstacle surfaces can be compared to the original field seen in Figure 1. The authors referred to this new obstacle surface repulsion as the "conveyor-belt function" and it is clear why as the modified vector field efficiently pulls the robot around the surface.

IV. Applications

The allure of using APFs is that they are computational inexpensive. This means that they can be run on smaller robots with less powerful on-board processors. APFs could be used in a number of practical applications if a reliable and widely applicable solution to the local minimum problem was found and implemented. Search and rescue operations in disaster zones could be conducted by swarms of robots using an APF exploration method to quickly explore damaged buildings, whose complex geometry would definitely cause issues with unmodified APFs. There would also have to be an object recognition AI process running on the robot to tag survivors or bodies it finds, but using an inexpensive exploration method would leave more processing power open for the AI process. There is also the obvious military application along the same idea: using a swarm of exploratory robots to scout dangerous buildings or structures thereby reducing the threat exposure of soldiers in war zones. These are just a few of the potential applications of a robust APF-based exploration algorithm.

V. Conclusion

Artificial Potential Fields are very useful in efficiently directing exploration efforts by autonomous agents. The major pitfall of this exploration method is the presence of local minimums that will permanently stop the exploration process without some adjustment. This paper presented the root cause of local minimums: the cancellation of attractive force vectors caused by a desirable goal location with the repulsive force vectors of nearby obstacles. The most common source of local minimums were seen to be concave structures [3]. Various, recently proposed, modifications to the basic APF framework were then covered with special focus on how they solved the local minimum problem inherent in APFs. In [1], when the exploration algorithm detected that the robot has been loitering in the same location for an extended amount of time, a virtual obstacle is placed at the robot's location with an increasingly repulsive magnitude. This virtual obstacle would eventually free the trapped robot so it could continue the exploration effort. In [2] and [3], rotation or vorticity was introduced into an object's repulsive field in order to direct the robot around it while also eliminating the major cause of local minimums. Each of these modified APFs succeeded in preventing a robot from being permanently trapped, but improvement and expansion is definitely possible. For example, if the method outlined in [3] was able to be extended into 3D exploration, then it could possibly be more efficient than the method proposed in [1]. The robot explorer in [1] was actually trapped for a short amount of time (Figure 2), whereas the robot in [3] never encountered a local minimum (Figure 5), despite the perfect conditions existing for a standard APF (Figure 1).

Another important improvement to APFs would be extending its use to dynamic environments. Addressing moving objects in the environment could potentially be done using a special repulsive field. The magnitude and direction of the field could be determined by the rate of change of its position between time steps. The larger the displacement, the stronger the repulsion force exerted by the field. Since there is a lot of uncertainty regarding the heading and future position of dynamic objects, an enlarged virtual obstacle could be created so that there is a "safe-zone" around the object that the robot would be repulsed from entering. This would extend the usability of APFs to the real-world where people, vehicles, animals, and other environmental elements are in motion and should be avoided by the exploring robot.

References

[1] C. Wang et al. Towards Autonomous Exploration with Information Potential Field in 3D Environments. In *Proceedings of the 2017 18th International Conference on Advanced Robotics (ICAR)*, 2017.

[2] D. McIntyre, W. Naeem, S.S.A. Ali, and A. Anwer. Underwater Surveying and Mapping using Rotational Potential Fields for Multiple Autonomous Vehicles. In *2016 IEEE 6th International Conference on Underwater System Technology: Theory & Applications*, 2016.

[3] A. Kenealy, N. Primiano, A. Keyes, D. Lyons. Thorough Exploration of Complex Environments with a Space-Based Potential Field. In *Proc. SPIE 9406, Intelligent Robots and Computer Vision XXXII: Algorithms and Techniques*, 2015.

[4] T. Liu and D. Lyons. Leveraging area bounds information for autonomous decentralized multi-robot exploration. In Robotics and Autonomous Systems, Vol 74, Part A, Pages 66-78, 2015.